

General Disclaimer

One or more of the Following Statements may affect this Document

- This document has been reproduced from the best copy furnished by the organizational source. It is being released in the interest of making available as much information as possible.
- This document may contain data, which exceeds the sheet parameters. It was furnished in this condition by the organizational source and is the best copy available.
- This document may contain tone-on-tone or color graphs, charts and/or pictures, which have been reproduced in black and white.
- This document is paginated as submitted by the original source.
- Portions of this document are not fully legible due to the historical nature of some of the material. However, it is the best reproduction available from the original submission.

**NASA TECHNICAL
MEMORANDUM**

NASA TM X-73416

NASA TM X-73416

(NASA-TM-X-73416) AERODYNAMIC PERFORMANCE
OF TWO VARIABLE-PITCH FAN STAGES (NASA)
12 p HC \$3.50 CSCI 01A

N76-26154

Unclas
G3/02 42389

AERODYNAMIC PERFORMANCE OF TWO VARIABLE-PITCH FAN STAGES

by Royce D. Moore and George Kovich
Lewis Research Center
Cleveland, Ohio 44135

TECHNICAL PAPER to be presented at
Tenth Congress of the International Council
of the Aeronautical Sciences sponsored by
the American Institute of Aeronautics and Astronautics
Ottawa, Canada, October 3-8, 1976



AERODYNAMIC PERFORMANCE OF TWO VARIABLE-PITCH FAN STAGES

Royce D. Moore and George Kovich
National Aeronautics and Space Administration
Lewis Research Center
Cleveland, Ohio 44135

ABSTRACT

NASA-Lewis Research Center is investigating a variety of fan-stages applicable for short-haul aircraft. These low-pressure-ratio low-speed fan stages may require variable-pitch rotor blades to provide optimum performance for the varied flight demands and for thrust reversal on landing. A number of the aerodynamic and structural compromises relating to the variable-pitch rotor blades will be discussed. This paper will present the aerodynamic performance of two variable-pitch fan stages operated at several rotor blade setting angles for both forward and reverse flow application. Detailed radial surveys are presented for both forward and reverse flow.

INTRODUCTION

The National Aeronautics and Space Administration in a coordinated effort with industry is investigating engines for powered-lift short-haul commercial aircraft application. In powered-lift systems, the engine thrust is used to assist the wing in producing the required lift for take-off from relatively short runways. The shorter runway capability requires aircraft with higher thrust engines and this ordinarily would mean noisier aircraft. However, there is a requirement that all future aircraft be quieter than the present ones.

A high bypass ratio engine offers the potential for a quiet powered-lift aircraft: The engine noise is relatively low; the jet velocity is moderate which results in reduced wing noise; and the exhaust temperature is low enough to be compatible with light-weight low-cost structural materials. In a high bypass ratio engine, the fan flow is large compared to that for the core compressor.

The powered-lift engines must also be capable of reversing the thrust after landing. The conventional engine thrust reverser consists of a vee-shaped target or a cascade of vanes mounted at the exhaust of the core to turn in the forward direction. For the high bypass ratio engines, large weight penalties could result if the cascade of vanes had to be added to the bypass duct to obtain the necessary reverse thrust for the short runways. A lighter-weight more-efficient method of reversing the thrust would be to use variable-pitch rotor blades similar to the reverse-pitch propeller. The air would be pulled from the rear of the engine and exhausted out of the nacelle inlet. Having incorporated the variable-pitch capability for reverse flow, it can be used to obtain optimum rotor blade setting angles for all engine operating conditions including take-off, cruise, and approach.

The Lewis Research Center has investigated a variety of fan stages for powered-lift engine application (refs. 1 to 10). There were two variable-pitch fan stages in the Lewis program. The design and performance of these two fans will be discussed in this paper. Both of the 51-centimeter diameter experimental fan stages incorporated provisions for

manual adjustment of the rotor blade setting angles. Tests were obtained at several angles to obtain both forward and reverse flow. Detailed flow surveys of pressure, flow angle, and temperature were obtained at each setting angle.

DESIGN COMPROMISES FOR VARIABLE-PITCH FANS

There are several design constraints which have to be considered in the design of variable-pitch fans. In addition to the requirements for high efficiency, adequate stall margin, and low noise which must also be met by fixed pitch fans, the variable-pitch fan must consider the following items:

1. Blade solidity. There are two possible methods for obtaining reverse flow through the fan as illustrated in figure 1. Obtaining reverse flow through flat pitch (fig. 1(b)) requires that the blade solidity be less than unity so that adjacent blades may rotate past each other without mechanical interference. In this case the blade turns such that the design leading edge of the blade is still the leading edge, but the blade camber is reversed with respect to the direction of flow and rotation. For operation through feather pitch (fig. 1(c)), the blade solidity can be greater than unity. In this case, the rotor trailing edge becomes the leading edge and the rotor blade camber remains proper with respect to the direction of flow and rotation.

2. Blade number. Since the fans will have relatively high flow compared to the core engine flow and therefore a low hub-tip radius ratio, the number of blades must be small (10 to 20) to accommodate a variable-pitch control mechanism. Unless the blades are flared in the tip region, the small blade number and low solidity results in insufficient blade chord to properly turn the flow and add the required energy.

3. Blade tip clearance. To allow the blades to turn, the rotor blade tip contour will basically be a circular arc shape. Thus the blade tip clearance will be minimum at the radial axis of blade rotation and considerably greater at the leading and trailing edges. Although not used with the present designs, a method for reducing the tip clearance at the leading and trailing edges would be to reshape the casing above the rotor tip to match the blade tip contour.

4. Blade thickness. The hub section of the blades may have to be thicker than would normally be desired. Since the low hub-tip radius ratio blades are adjustable, no part-span vibration dampers can be used. Thus relatively thicker hub sections are required to accommodate the blade stresses.

APPARATUS AND PROCEDURE

Test Stages

The aerodynamic design of the test stages is

presented in references 1 and 6. Thus only a brief description of each stage is given herein. Flow paths for both stages are presented in figure 3 and photographs of the rotors and stators are presented in figure 3.

Stage 51B (ref. 6) was designed for a pressure ratio of 1.15 at a tip speed of 243 meters per second and a flow of 28.9 kilograms per second (175.8 Kg/sec/m² of annulus area). The rotor blade solidity varied from 0.65 at the tip to 0.98 at the hub so that reverse flow could be obtained through both flat and feather pitch. The rotor had 12 blades and had a hub-tip radius ratio of 0.4. The 32 stator blades were spaced two rotor tip chords downstream of the rotor. Both the rotor and stator blades utilized double-circular-arc blade profiles. Some design blade element parameters for Rotor 51B are presented in table I(a).

Stage 55 (ref. 1) was designed for a pressure ratio of 1.20 at a tip speed of 213 meters per second and a flow of 31.2 kilograms per second (195.3 Kg/sec/m² of annulus area). The rotor had 15 blades with a hub-tip radius ratio of 0.46. The rotor blade solidity varied from 0.89 at the tip to 1.22 at the hub. Since the hub solidity was greater than unity, reverse flow could only be obtained with rotation through feather pitch. This rotor also utilized double-circular-arc blade profiles. A few of the design blade-element parameters for Rotor 55 are listed in table I(b). The 11 stator blades used NACA-400-series airfoils (ref. 11).

Both stages were designed with adjustable rotor blades. The convention of blade setting angle is illustrated in figure 1. For forward flow (fig. 1(a)), the flow enters the rotor and exits through the stator. Blade setting angles are measured from the design setting angle and are positive when the leading edge is turned toward the direction of rotor rotation. For reverse flow (figs. 1(b) and (c)), the stator becomes an inlet guide vane. Turning the blades through feather means the blades move in the negative direction; turning the blades through flat pitch corresponds to the positive direction.

Test Facility

The fan stages were tested in the Lewis Single-Stage Compressor Test Facility. A schematic diagram of the facility is shown in figure 4. For the forward flow tests, atmospheric air enters the test facility at an inlet located on the roof of the building, flows through the orifice, and into the plenum chamber upstream of the test stage. The air then passes through the experimental stage into the collector and is exhausted to the facility exhaust system. Flow rate was varied by controlling the collector throttle valve.

For the reverse flow tests, the two 90-degree elbows were removed from the sides of the cylindrical collector. Air was drawn from the room into the collector and traveled the reverse direction to the inlet on the roof. Flow rate was varied by controlling the inlet throttle valve. The collector valve was fully open for the reverse flow tests.

Instrumentation

Radial surveys of the flow were made at three

axial stations for each stage (see fig. 2). At each measuring station, two combination probes and two 8° wedge probes were used (fig. 5). Each probe was positioned with a null-balancing, stream-directional sensitive control system that automatically aligned the probe to the direction of the flow. The total pressure, total temperature, and flow angle were determined using the combination probe (fig. 5(a)) and the static pressure was measured by the wedge probe (fig. 5(b)).

An electronic speed counter, in conjunction with a magnetic pickup, was used to measure rotational speed. Flow rate was determined from a calibrated orifice.

RESULTS AND DISCUSSION

The overall stage performance for both stages will be presented first for forward flow and with the rotor blades at the design setting angle. The effect of changes in rotor setting angle on the forward flow performance is presented. Overall performance and radial distributions of performance are discussed. The effects of blade setting angle on reverse flow performance and values of calculated thrust are presented.

Overall Performance at Design Angle

The overall stage performance for both stages are presented for forward flow and the rotor blades at design setting angle in figure 6. Pressure ratio and adiabatic efficiency are presented as functions of equivalent airflow for speeds from 80 to 120 percent of design. The design point is shown as the solid symbol. For both stages, the measured pressure ratio was less than the design value. Peak efficiency decreased with increasing speed for both stages. At design flow and speed, the efficiency for stage 51B is 0.89. Peak efficiency is 0.92 at design speed and occurs at a greater than design flow. For stage 55, peak efficiency is 0.87 at design speed and occurs at less than design flow.

Effect of Blade Setting Angle on Forward Flow Performance

The effect of rotor blade setting angle on the overall stage performance is presented in figure 7 for design speed and forward flow conditions. For both stages, the rotor blades were reset at both positive and negative angles from the design setting angle. Turning the blades to a more positive angle tends to close the blade passages and reduce the flow whereas a negative setting angle opens the blade passages and increases airflow. As the rotor blades were opened (going from positive to negative angles), the overall pressure ratio increased and the peak efficiency decreased for both stages. These effects are present across the entire blade span as illustrated in figure 8. Rotor pressure ratio and adiabatic efficiency are plotted as a function of percent span from tip for the three blade setting angles. For each setting angle, the data for the test point which gave peak efficiency at design speed are plotted. At each percent-span location, the pressure ratio increased with decreasing setting angle. Efficiency decreased with decreasing setting angle.

Effect of Blade Setting Angle on Reverse Flow Performance

Typical overall performance for the stages operating with reverse flow is presented in figure 9. The setting angles presented were obtained by rotating the blades through feather pitch. For both stages, data are presented for 80, 90, and 100 percent of design speed. For the reverse flow, the pressure ratio is that from station 5 to station 1 (see Fig. 8). In reverse operation, the stage demonstrates the same trends of increasing flow and pressure ratio with increasing speed as with forward flow. Although the pressure ratio is approximately the same as the design value with forward flow, the airflow is approximately half the design value.

A comparison of the outlet pressure distribution for forward and reverse flows is given in figure 10 for stage 55. Although the overall pressure ratio was approximately the same for both flows, the radial distributions of downstream total pressure are quite different. For the forward flow, the pressure gradually decreases toward the hub. For the reverse flow, total pressure decreases rapidly from the tip to the 70-percent span and then is essentially equal to the static pressure from there to the hub. The equal total and static pressures in the hub region of the rotor indicate negligible velocity or flow. For the reverse flow setting angle the blade profile in the hub region was approximately perpendicular to the axial direction. This blade orientation tends to block flow. For all reverse flow conditions, the hub region had essentially no flow. The extent of the affected region was dependent on the setting angle.

Effect of Blade Setting Angle on Thrust

One purpose of the variable-pitch rotor blade is to provide the optimum performance for the various operation requirements including take-off, cruise, approach, and reverse thrust. The effect of rotor blade setting angle on the maximum calculated thrust at design speed is shown in figure 11 for both stages in the test model size. Since the shape of the curve was unknown between the positive and negative thrust points, a dashed line was used to connect these groups of points. For the forward flow setting angles tested, thrust increased with decrease in angle.

Reverse flow was obtained for stage 51B both by increasing setting angle (rotating through flat pitch) and by decreasing setting angle (through feather pitch). For stage 55, reverse thrust was obtained through feather only (decrease angle). The calculated negative thrust values obtained through feather were more than double those obtained through flat pitch. This is probably due to the reverse blade camber when the blades are turned through flat pitch. For stage 51B, there appears to be an optimum setting angle for maximum reverse thrust. At the setting angle of design minus 95°, the reverse thrust value was the largest. For both stages, reverse thrust values greater than 50 percent of the design forward flow values were obtained.

CONCLUSIONS

The aerodynamic performance for two fan stages having variable-pitch rotors has been presented.

The 51-centimeter diameter fans were tested at blade setting angles which produced forward flow and reverse flow. Satisfactory performance was obtained with both of these fans. The pressure ratio for reverse flow was approximately the same as that for forward flow; however, the airflow was about one-half the forward airflow.

It was found that adequate reverse thrust (more than 50 percent of the forward design thrust) can be obtained with variable-pitch rotors. Reverse thrust values obtained for blade rotation through feather were much higher than those obtained for rotation through flat pitch. This was attributed to the reverse blade camber for rotation through flat pitch. Radial surveys of pressure with reverse flow indicates little or no flow in the inner third of the exit passage.

REFERENCES

1. Lewis, G. W., Jr., Moore, R. D., and Kovich, G., "Performance of a 1.20 Pressure-Ratio STOL Fan Stage at Three Rotor Blade Setting Angles," TM X-2857, 1973, NASA.
2. Lewis, G. W., Jr., and Tysl, E. R., "Overall and Blade-Element Performance of a 1.20-Pressure-Ratio Fan Stage at Design Blade Setting Angle," TM X-3101, 1974, NASA.
3. Lewis, G. W., Jr., Osborn, W. M., and Moore, R. D., "Overall and Blade-Element Performance of a 1.20-Pressure Ratio Fan Stage with Rotor Blades Reset Design Minus 5 Degrees," TM X-3338, 1976, NASA.
4. Lewis, G. W., Jr. and Kovich, G., "Overall and Blade-Element Performance of a 1.20-Pressure Ratio Fan Stage with Rotor Blades Reset Design Minus 7 Degrees," TM X-3342, 1976, NASA.
5. Osborn, W. M. and Steinke, R. J., "Performance of a 1.15 Pressure Ratio Axial-Flow Fan Stage with a Blade Tip Solidity of 0.5," TM X-3052, 1974, NASA.
6. Kovich, G. and Steinke, R. J., "Performance of a 1.15 Pressure Ratio Axial-Flow Fan Stage with a Blade Tip Solidity of 0.65," TM X-3341, 1976, NASA.
7. Moore, R. D. and Steinke, R. J., "Aerodynamic Performance of a 1.25 Pressure-Ratio Axial-Flow Fan Stage," TM X-3083, 1974, NASA.
8. Kovich, G., Tysl, Ed. R., and Moore, R. D., "Performance of a Low-Pressure Ratio Fan Stage at Several Off-Design Blade Setting Angles." Proposed NASA Technical Memorandum.
9. Kovich, G. and Moore, R. D., "Reverse Flow Performance of a Low-Pressure Ratio Fan Stage at Several Rotor Blade Setting Angles." Proposed NASA Technical Memorandum.
10. Moore, R. D., Lewis, G. W., Jr., and Tysl, E. R., "Performance of a Low-Pressure Fan Stage with Reverse Flow," TM X-3349, 1976, NASA.

11. Jacobs, E. N., Ward, K. E., and Pinkerton, R. M., "The Characteristics of 76 Related Airfoil Sections from Tests in the Variable-Density Wind Tunnel," TR-400, 1933, NACA.

TABLE I. - DESIGN BLADE-ELEMENT PARAMETERS

(a) Rotor S1R

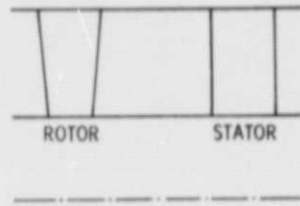
	Tip	Mean	Hub
Inlet radius, cm	25.40	17.51	10.18
Inlet Mach number	0.51	0.50	0.46
Diffusion factor	0.40	0.47	0.47
Chord, cm	8.63	6.91	5.23
Solidity	0.65	0.75	0.98
Inlet blade angle, deg	56.3	44.5	27.3
Blade camber, deg	13.0	23.3	30.0

(b) Rotor 55

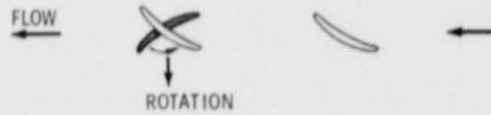
	Tip	Mean	Hub
Inlet radius, cm	25.40	18.32	11.68
Inlet Mach number	0.58	0.55	0.56
Diffusion factor	0.44	0.50	0.53
Chord, cm	9.50	7.70	5.97
Solidity	0.89	1.00	1.22
Inlet blade angle, deg	50.4	44.0	28.1
Blade camber, deg	18.4	30.6	44.9

ER

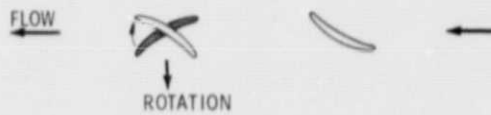
ORIGINAL PAGE IS
OF POOR QUALITY



(a) FORWARD FLOW.



(b) REVERSE FLOW BY ROTATION THROUGH FLAT PITCH.



(c) REVERSE FLOW BY ROTATION THROUGH FEATHER PITCH.

Figure 1. - Blade orientation.

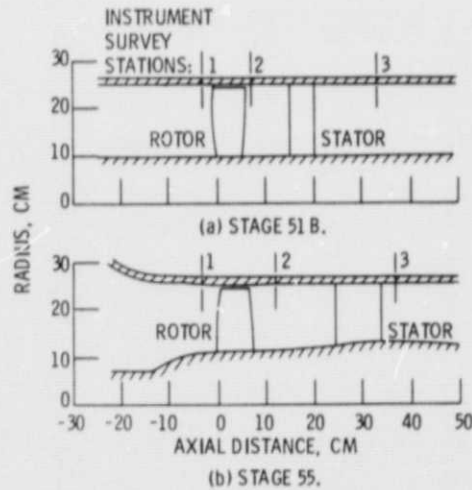
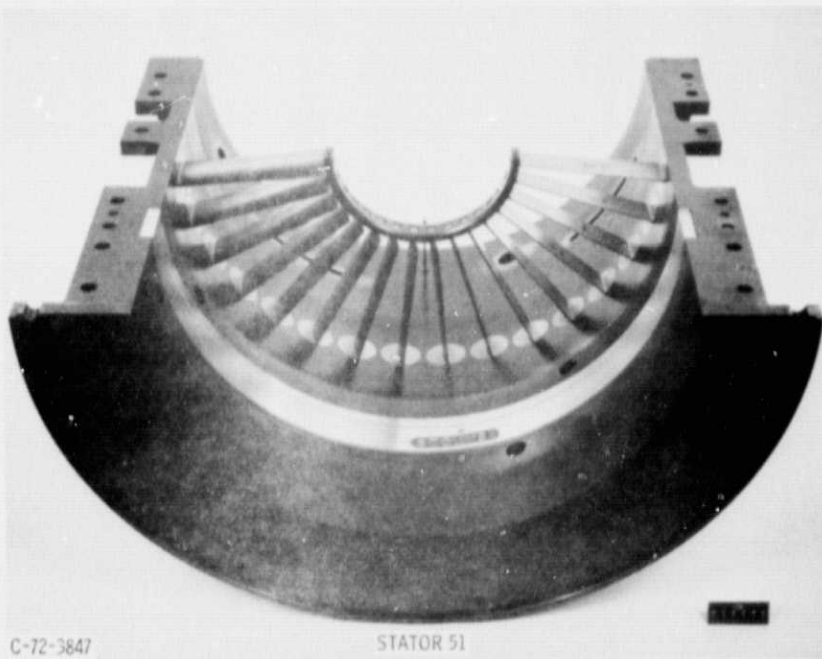
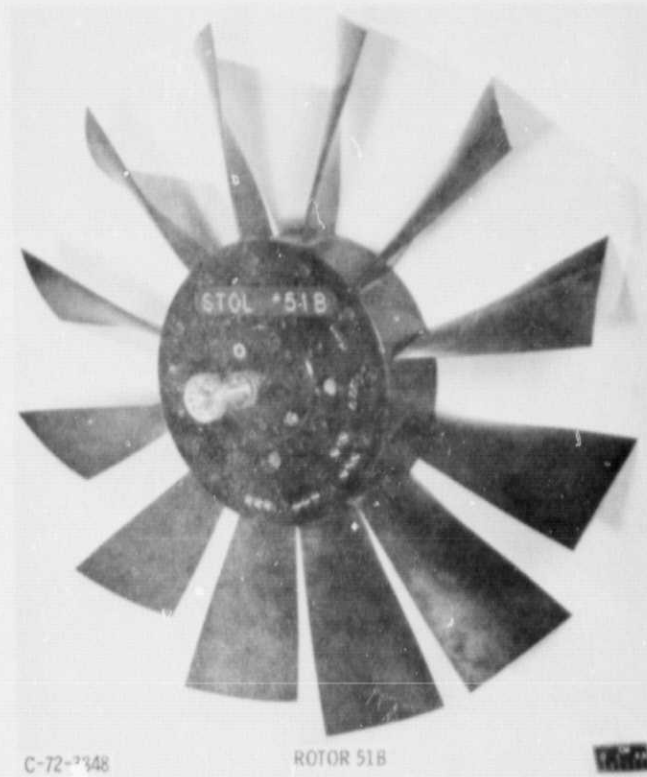


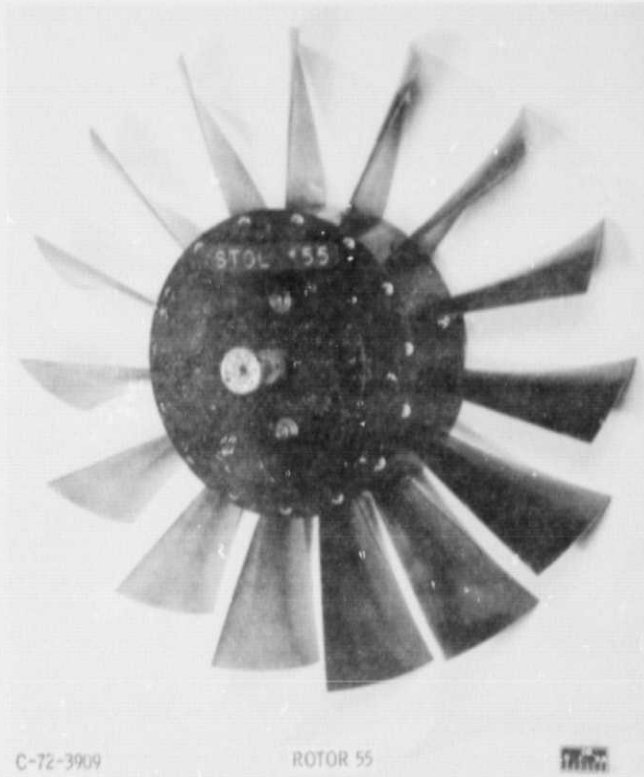
Figure 2. - Flow paths showing instrumentation locations.

8-6658



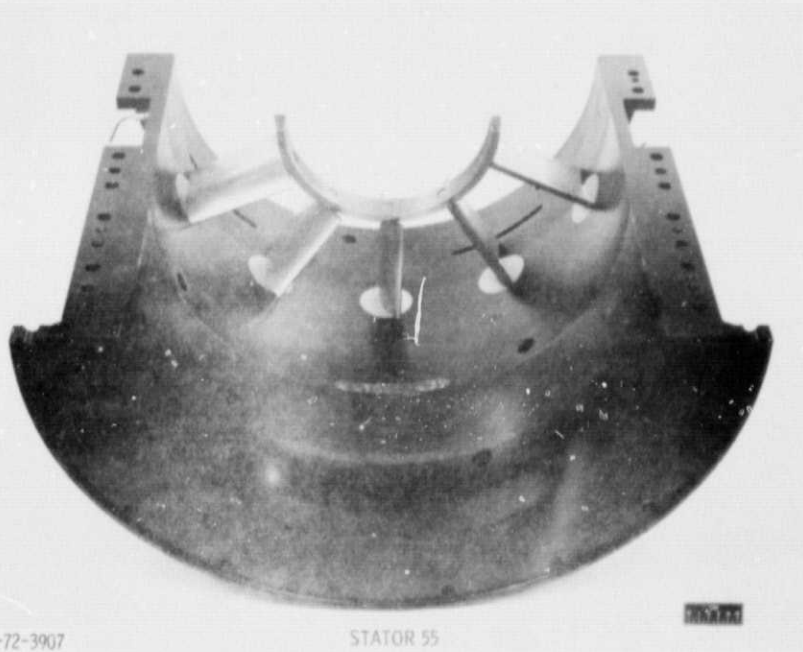
(a) STAGE 51B.
Figure 3. - Fan stages.

PRECEDING PAGE BLANK NOT FILMED



C-72-3909

ROTOR 55



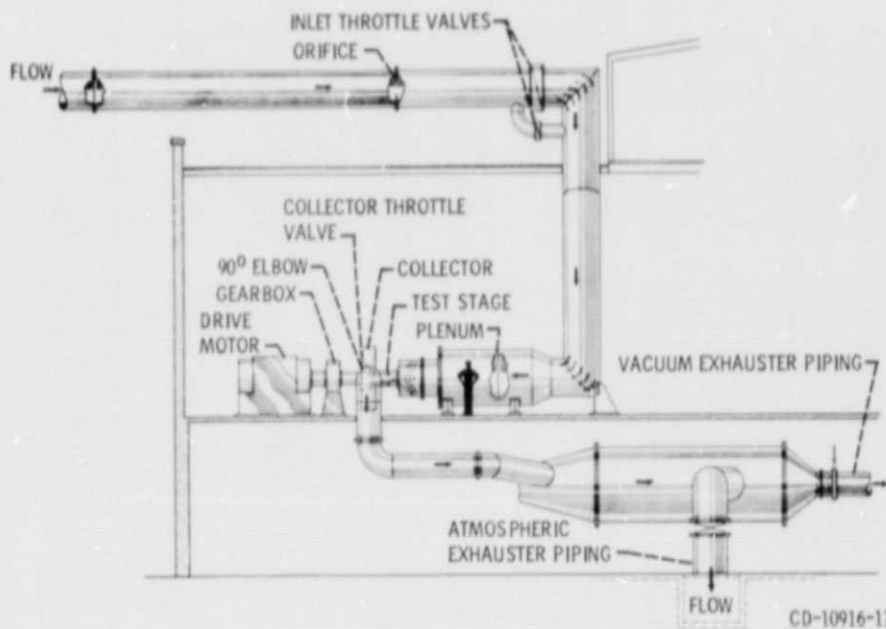
C-72-3907

STATOR 55

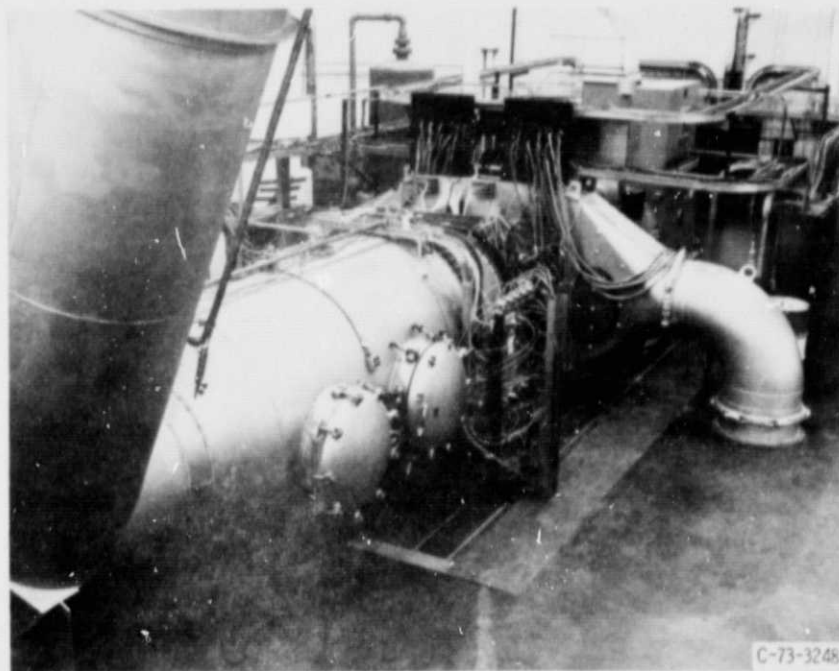


(b) STAGE 55.

Figure 3. - Concluded.

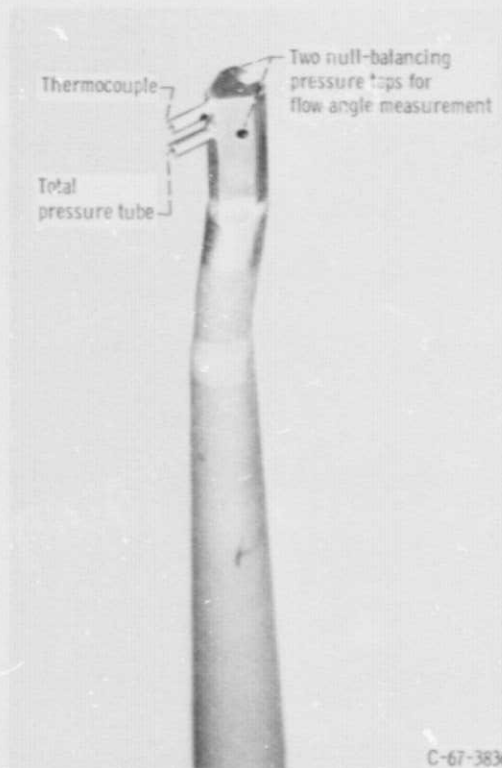


(a) SCHEMATIC.

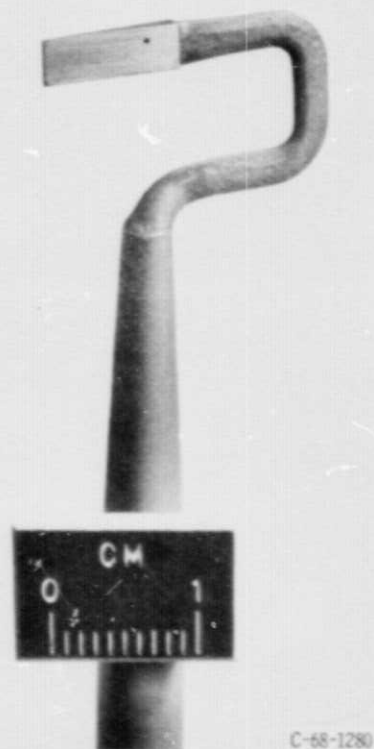


(b) PHOTOGRAPH.

Figure 4. - Compressor test facility.



(a) Combination total pressure, total temperature, and flow angle probe.



(b) Static pressure probe; 8° C-shaped wedge.

Figure 5. - Survey probes.

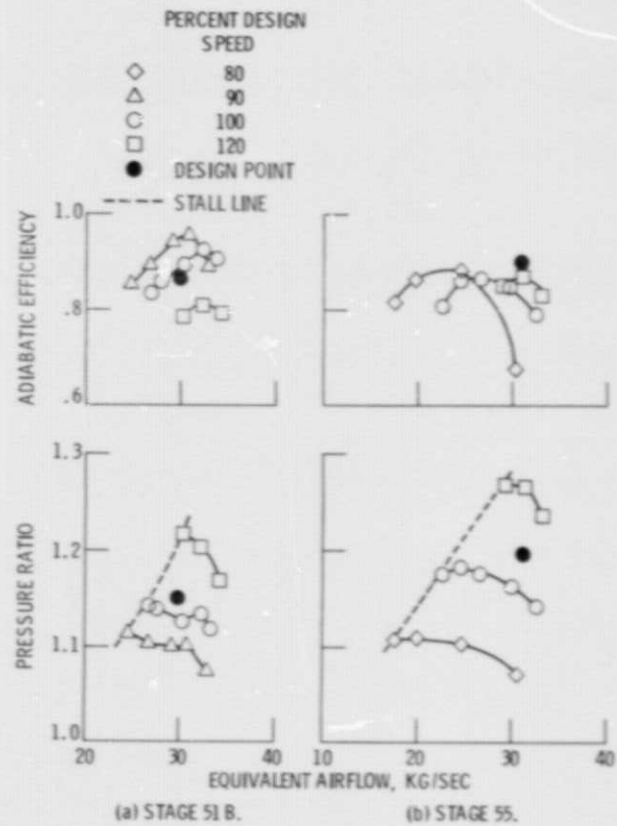


Figure 6. - Overall stage performance with rotor blades at design angle.

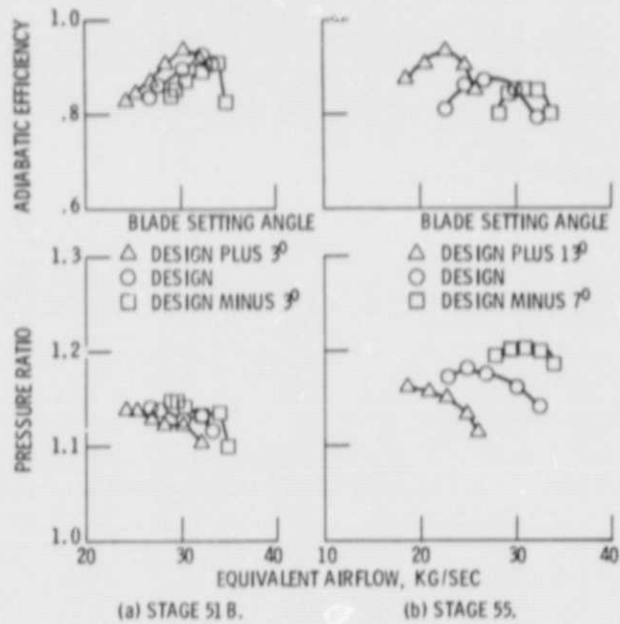


Figure 7. - Effect of blade setting angle on overall stage performance. Design speed; forward flow.

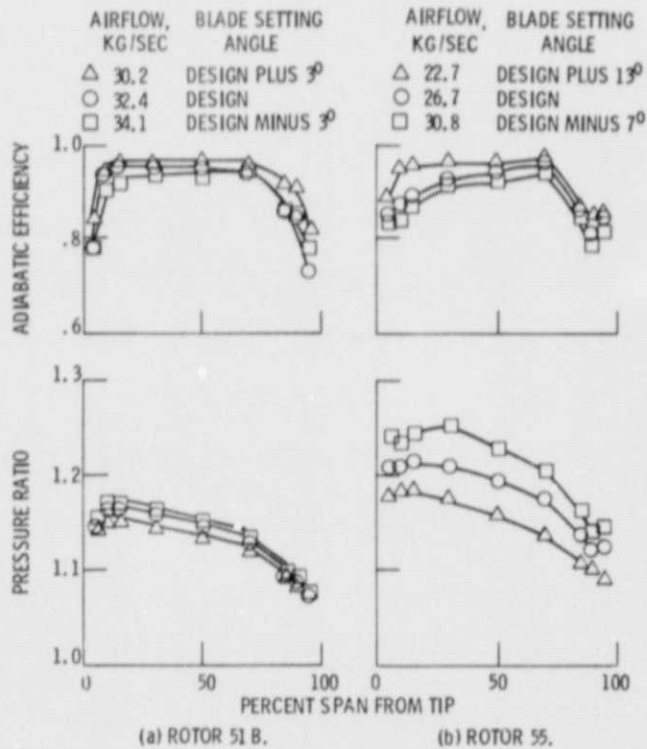


Figure 8. - Effect of blade setting angle on radial distribution of performance. Design speed; forward flow.

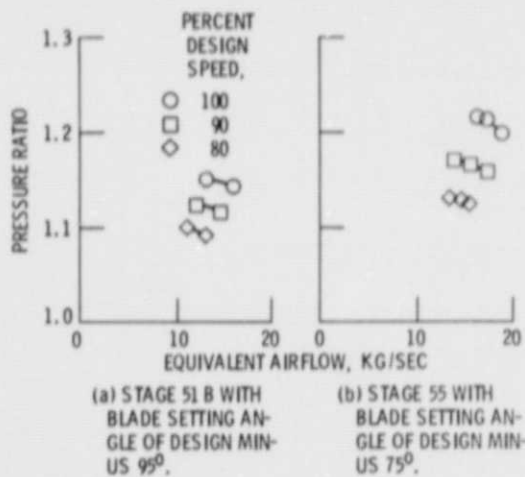


Figure 9. - Overall pressure ratio with reverse flow.

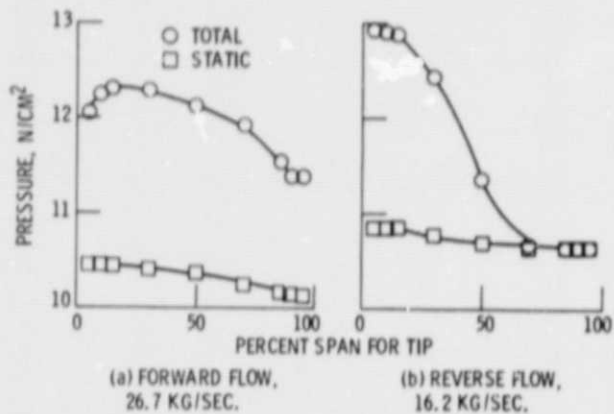


Figure 10. - Comparison of outlet pressure distributions for forward and reverse flow. Stage 55.

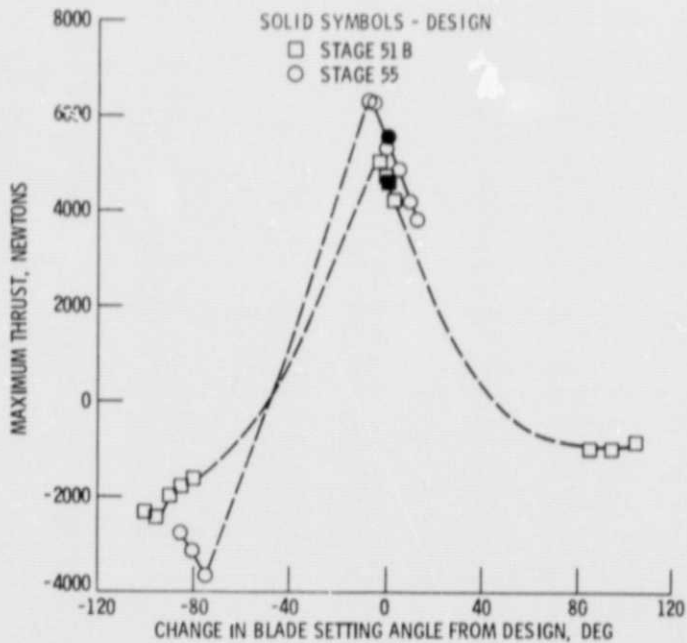


Figure 11. - Effect of blade setting angle on thrust. Design speed.